

Crack Depth Evaluation for Boiler Tubes using X-ray Image Analysis

Masaaki Torichigai^{*1}Hirotohi Matsumoto^{*1}Takeshi Miyazawa^{*2}Satoshi Chaen^{*3}Kyoko Wada^{*4}

Since there are no effective methods available, corrosion fatigue cracks occurring at the back side of the attachment weld portion on the boiler furnace wall (tube interior) have so far been examined by sampling from the removed tube. For this reason, it took time for evaluation, as well as cost for tube extraction and restoration. Hence, focusing on the X-ray inspection that has seen recent rapid progress, Mitsubishi Heavy Industries, Ltd. has established a technology which detects a variety of cracks including corrosion fatigue by processing digitized X-ray images to evaluate the crack depth from the luminance difference between sound metal and the cracked zone. This has permitted on-site judgment of replacement, substantially lowering the evaluation cost resulting from unnecessary tube extraction and restoration.

1. Introduction

Digital X-ray equipment is, depending upon the type of detector used in place of photographic film, divided into X-ray TVs (image intensifier-attached TV camera), flat-panel semiconductor image detectors (Flat Panel Detector: FPD), and photo-stimulable phosphor image detectors (imaging plate-based Computed Radiography: CR). The greatest advantage of digital X-rays is possible real-time or quick judgment on results and image preservation/transmission is also easy. It is further said that, due to the enhanced performance of detectors and the development of image processing technology with the progress of computers, resolution is also reaching a level favorably comparing with that of X-ray films, and recent years have come to witness rapid prevalence. That is why the author et al. also tried to apply digital X-ray approaches to a variety of cracks occurring to thermal power plants and found a film method superior in terms of detection limits.

We have thus established and introduce a technology to quantitatively evaluate the depth of invisible cracks which occur at the back side of the attachment weld portion along the boiler furnace wall tube (tube interior), as well as circumferential cracking, etc., occurring in the same furnace wall tube in the crown (top) part of the furnace by digitizing and image-processing the X-ray inspection results.

2. Comparison between CR Process and film method

Fig. 1 compares the detection limits of the CR (Computed Radiography) process and a film method by which a 0.1mm-wide and a 0.5-2.0mm-deep slit processed on the outer surface of a generating tube ($\phi 28.6 \times t 6.5 \text{mm}$) was photographed. As shown in the figure, the film method could detect down to a 0.5mm-deep slit while the CR process could not detect a 0.5mm-deep slit. With respect to the images themselves, the film method's images are also clearer than the CR process.

3. Application to corrosion fatigue cracks

If a boiler is operated for many hours, corrosion fatigue cracks occur on the inner surface of the furnace wall tube around the attachment weld portion. Since these cracks occur at the reverse

*1 Nagasaki Research & Development Center

*2 Boiler Engineering Department, Power Systems

*3 Takasago Research & Development Center

*4 Advanced Technology Research Center

side of the weld bead as shown in **Fig. 2**, ultrasonic inspection of sections where only an ultrasonic probe can be applied is conducted, but there is no effective method of inspection.

For this reason, we considered the detection of corrosion fatigue cracks through the use of X-rays and how the depth should be evaluated.

3.1 Inspection outline and specimen

Fig. 3 shows an outline of X-ray inspection. On the surface of the tube inside the furnace, an X-ray film is attached to be X-rayed from outside the furnace (attachment weld side).

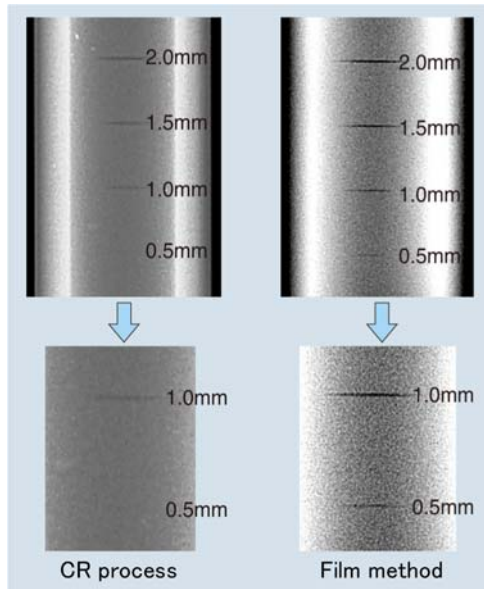


Figure 1 Comparison between CR Process and Film Method

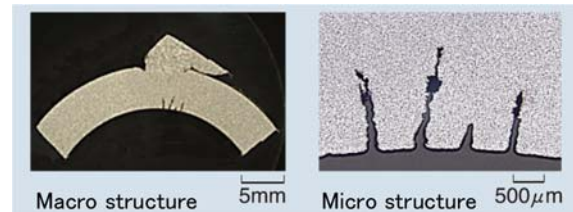


Figure 2 Example of Corrosion Fatigue Cracks

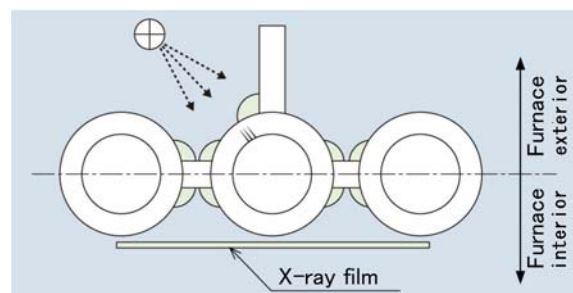


Figure 3 Outline of X-Ray Inspection

Fig. 4 and **Fig. 5** show the appearance of a specimen. On a $\phi 28.6 \times t 6.5$ mm generating tube, weld bead-simulated 4, 5, 6, and 7mm-high weld deposits of 8mm in radius of curvature were TIG-welded and, on the tube's inner surface, a 0.1mm-wide and 0.4-2.0mm-deep slit was processed with a special thin cutter. Since the opening width of the corrosion fatigue cracks occurring to the boiler furnace wall tube is from 0.1-0.3mm, corrosion fatigue cracks on the furnace wall tube can be detected if the 0.1mm-wide slit processed on a specimen can be detected (with X-rays).

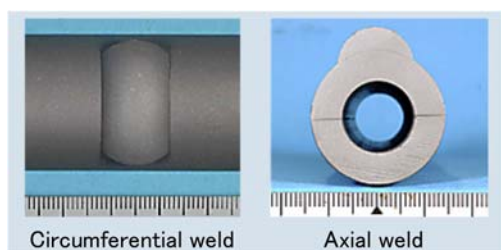


Figure 4 Appearance of Specimen

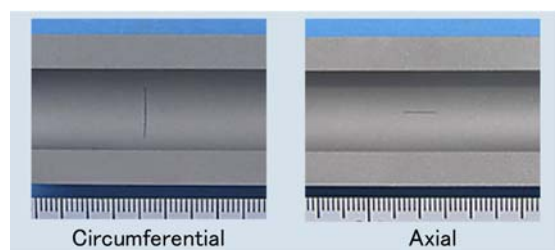


Figure 5 Appearance of Artificial Slit (Typical Example)

3.2 Test Results

Table 1 shows the test results for an axial slit. The results were about the same for both smooth and rifled tubes. If the bead was 5mm or less in height, slits of 0.4mm in depth could be detected. If the bead's height was 7mm or less, 0.5mm slits could be detected on both tubes.

Table 2 shows the test results for a circumferential slit. The results were about the same for both smooth and rifled tubes, and if the bead was 6mm or less in height, slits of 0.4mm in depth could be detected. If the bead's height was 7mm or less, 0.5mm slits could be detected on both tubes.

Table 1 Test Results for Axial Slit

Height of metal (height of bead)	Depth of slit (mm)			
	Smooth tube		Rifled tube	
	0.4	0.5	0.4	0.5
4mm	○	○	○	○
5mm	○	○	○	○
6mm	×	○	×	○
7mm	×	○	×	○

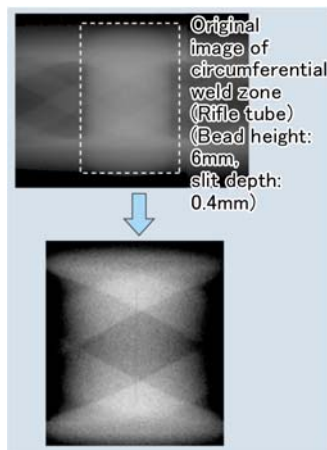
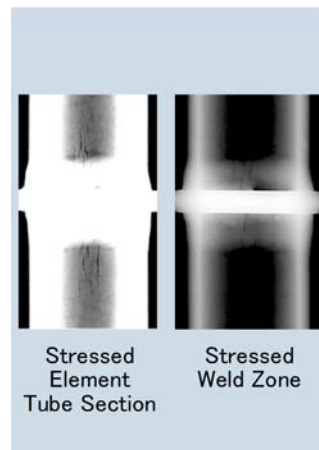
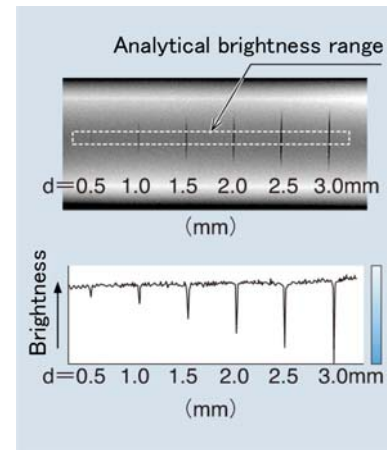
Table 2 Test Results for Circumferential Slit

Height of metal (height of bead)	Depth of slit (mm)			
	Smooth tube		Rifled tube	
	0.4	0.5	0.4	0.5
4mm	○	○	○	○
5mm	○	○	○	○
6mm	×	○	*○	○
7mm	×	○	×	○

*Graphics-processed images are inserted in the text.

Fig. 6 shows slit images optimized by image-processing. These images are X-ray images of a 0.1mm-wide and 0.4mm-deep slit processed on the inside surface of a circumferential weld zone with a bead height of 6mm. The desired range to be stressed (desired) is selected and, by narrowing or widening the range's contrast/gradation (γ value) or adjusting the brightness and contrast with a torn curve, the defect is highlighted. This helps us find even defects hard for the human eye to discern.

Fig. 7 shows X-ray images of corrosion fatigue cracks that occurred to an actual boiler. Since the element tube section and the weld zone have different levels of brightness, it is difficult to observe them at the same time. It can, however, be observed in detail how corrosion fatigue cracks occur if the element tube section and the weld zone are both optimized by image-processing.

**Figure 6 Optimized Image****Figure 7 X-Ray Image of Corrosion Fatigue Cracks****Figure 8 Measurement Results for Axial Brightness**

3.3 Evaluation of crack depth

Digitizing X-ray film images and measuring luminance difference between the sound and the cracked part permit the depth of cracks to be evaluated. **Fig. 8** shows the measurement results for the brightness of 0.5, 1.0, 1.5, 2.0, 2.5, and 3.0mm-deep artificial slits of 0.1mm in width processed in the circumferential direction on the outer surface of a generating tube ($\phi 28.6 \times t 6.5$ mm). These results show an axial change in brightness within the analytical range selected (as indicated with a dotted line in the photo), with the abscissa being for the axial range selected and the ordinate for brightness. As for the figure, around the axial center selected, the axial distribution of brightness taken indicates a change in brightness dependent upon the slit depth and the depth of cracks can be evaluated if the relationship between the amount of change and the depth of cracks is determined.

Fig. 9 shows the measurement results for the brightness of (3) 0.5, 1.0, and 1.5mm depth circumferential slits of 0.1mm in width processed on the inner surface of a circumferential weld zone. Taking the axial brightness distribution in a similar manner to that of Fig. 8, it is found that the brightness changes along the curvature of the weld bead. And since a circumferential slit was processed in the center of the weld bead on the tube's inner surface side (back side) to find a change in brightness corresponding to slit depth, it is also possible to evaluate the depth of the defect occurring to the weld zone.

Fig. 10 and **Fig. 11** show the relationship between slit depth and luminance difference determined for the element tube section of a generating tube ($\phi 28.6 \times t 6.5$ mm), as well as axial and circumferential weld zones with bead heights of 4, 5, 6, and 7mm. As seen from these figures, the

higher the weld bead of both the axial and circumferential weld zones, the smaller is the luminance difference, while there is a certain relationship identified between slit depth and luminance difference. Then, regarding the axial and circumferential weld zones, the relationship between the change in brightness with slit depth and X-ray penetration thickness (thickness \times 2+bead height) was determined so that the depth of corrosion fatigue cracks can be evaluated. Fig. 12 plots the evaluation accuracy for slits processed on the inner surface of the weld zone, proving that the depth of a defect on both axial and circumferential weld zones can be evaluated with ± 0.3 mm precision.

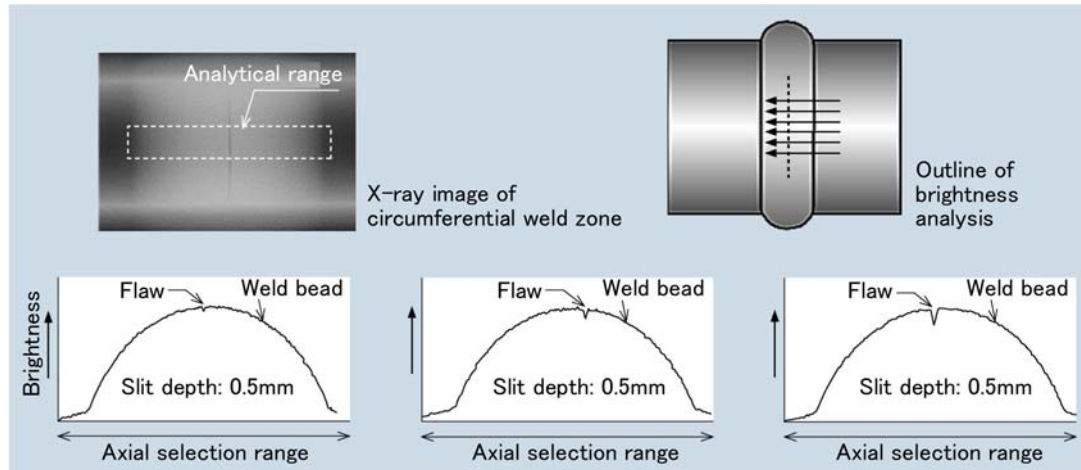


Figure 9 Evaluation of Defect Depth

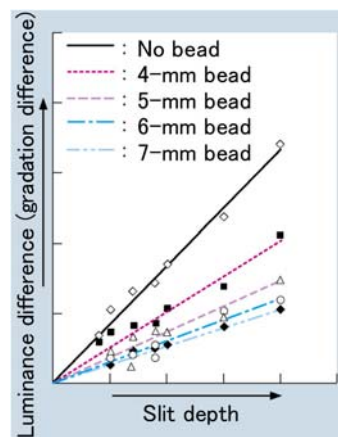


Figure 10 Relationship between Slit Depth and Luminance Difference (Axial Weld Zone)

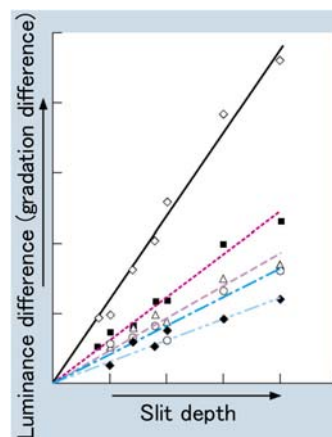


Figure 11 Relationship between Slit Depth and Luminance Difference (Circumferential Weld Zone)

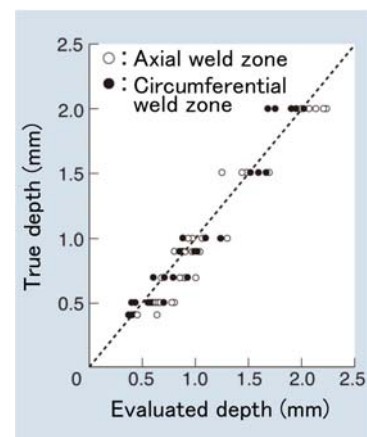


Figure 12 Evaluation Accuracy for Defects on Inner Surface of Tube

4. Circumferential Cracking Application

Fig. 13 shows the appearance and a cross-sectional view of circumferential cracking occurring on the surface of a coal-fired boiler furnace tube. In respect to the evaluation of circumferential cracking depth, despite a variety of inspection methods so far applied, dense cracks have prevented thorough evaluation. This is why the evaluation of circumferential cracking depth with X-rays was reviewed.

4.1 Detection limits

Fig. 14 shows the result of detection limit verification using circumferential cracks in an actual furnace wall tube. The circumferential cracking shown in the figure is minor and crack surface examination found the depth of crack A and crack B to be 0.53mm and 0.57mm, respectively. As seen from the comparison between the appearance and X-ray images, digitizing and image-processing the X-ray film permitted crack A and crack B to be detected and, if 0.5mm or more-deep circumferential cracking, it is fully detectable.

4.2 Evaluation of circumferential crack depth

If, like in corrosion fatigue cracks, the analytical range is selected and axial (orthogonal to

cracks) changes in brightness are measured, the depth of circumferential cracking can be determined since the brightness changes with the depth of the circumferential cracking.

Fig. 15 shows the evaluation accuracy for the circumferential cracking. As shown in the figure, measuring the luminance difference between the sound and the cracked section permits circumferential cracking depth to be evaluated with $\pm 0.3\text{mm}$ precision.

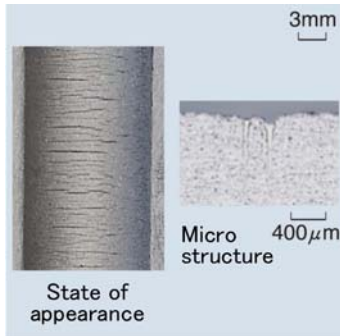


Figure 13 Appearance and cross-sectional state of circumferential cracking

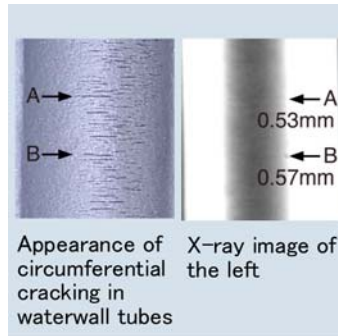


Figure 14 Detection limits for circumferential cracking

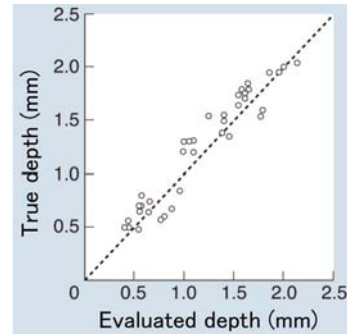


Figure 15 Evaluation accuracy for circumferential cracking

5. Evaluation of pitting corrosion

There are cases where pitting corrosion occurs on the undersurface of a transversal panel and pitting depth was evaluated with X-rays. Fig. 16 shows an X-ray image of the specimen for pitting evaluation and the measurement results for the brightness of the pitting zone (artificial flaws), indicating that the brightness changes with pitting depth. If the relationship between pitting depth and luminance difference has been determined, by using a specimen with the same specifications as those for the boiler tube to be evaluated, pitting depth can also be evaluated.

6. Actual applications

Table 3 shows the actual application history for field inspection. Circumferential cracking is hard to evaluate using other inspection methods, due to the occurrence of numerous cracks, thermal fatigue cracks that appeared on broad fins, cracks due to thermal shock in drain piping, and pitting corrosion on the transversal panel. Targeting the evaluation of corrosion fatigue cracks occurring to the back side of the attachment weld portion along the furnace wall tube (tube interior), our approach has been applied to a total of 11 boilers as of March 2011 since its first application to an actual plant in March 2006.

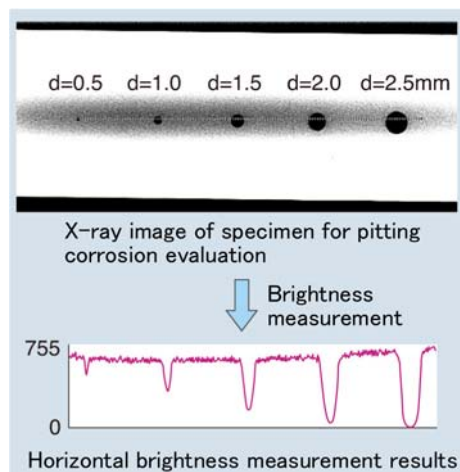


Figure 16 Evaluation of Pitting Depth

Table 3 Applications to Actual Plants

	Evaluation target	Number of boilers
①	Furnace wall corrosion fatigue crack inspection	4
②	Furnace wall circumferential cracking inspection	3
③	Furnace wall corrosion fatigue crack inspection	1
④	Drain pipe thermal shock crack inspection	1
⑤	Reheater pitting depth inspection	1
⑥	Superheater/reheater circumferential cracking inspection	1
	(Total)	11

7. Conclusion

This report has introduced an X-ray depth evaluation method for a variety of flaws including cracks occurring to a boiler tube. Toward the future, we intend to make similar efforts based on the above achievements for cracks and flaws occurring in other products as well in an attempt to widen applications of this technology.